Supporting Information

Nanostructured rhenium-carbon composites as hydrogen-evolving catalysts effective over the entire pH range

Minju Kim,[1,2] Zhijie Yang,[1] Jun Heuk Park,[1,2] Seok Min Yoon,[,1] and Bartosz A. Grzybowski*[,1,2]*

[1]Center for Soft and Living Matter, Institute for Basic Science (IBS), Ulsan 44919, Republic of Korea

[2]Department of Chemistry, Ulsan National Institute of Science and Technology (UNIST), Ulsan 44919, Republic of Korea

E-mail: smyoon1@wku.ac.kr, grzybor72@unist.ac.kr

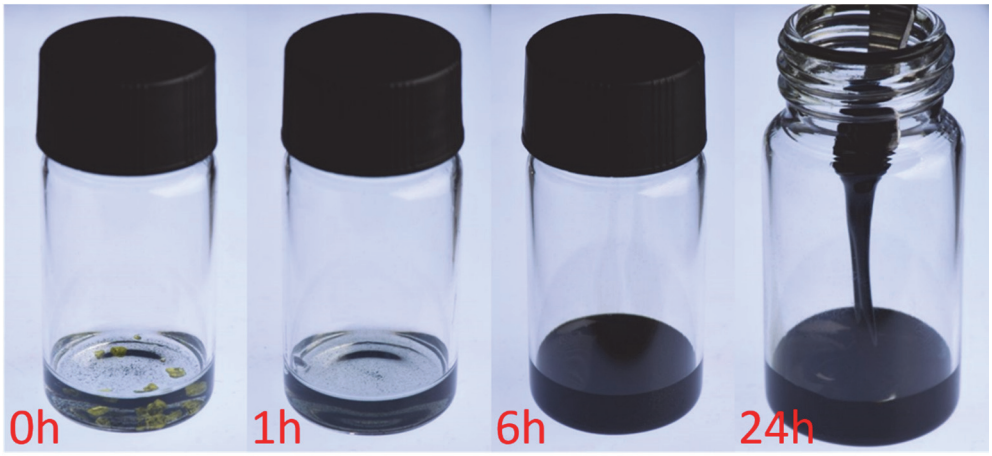

Figure S1. Photographs illustrating spontaneous sol-gel reaction taking place upon dissolving Re_2O_7 in THF and leading to Re_2O_7-poly(THF).

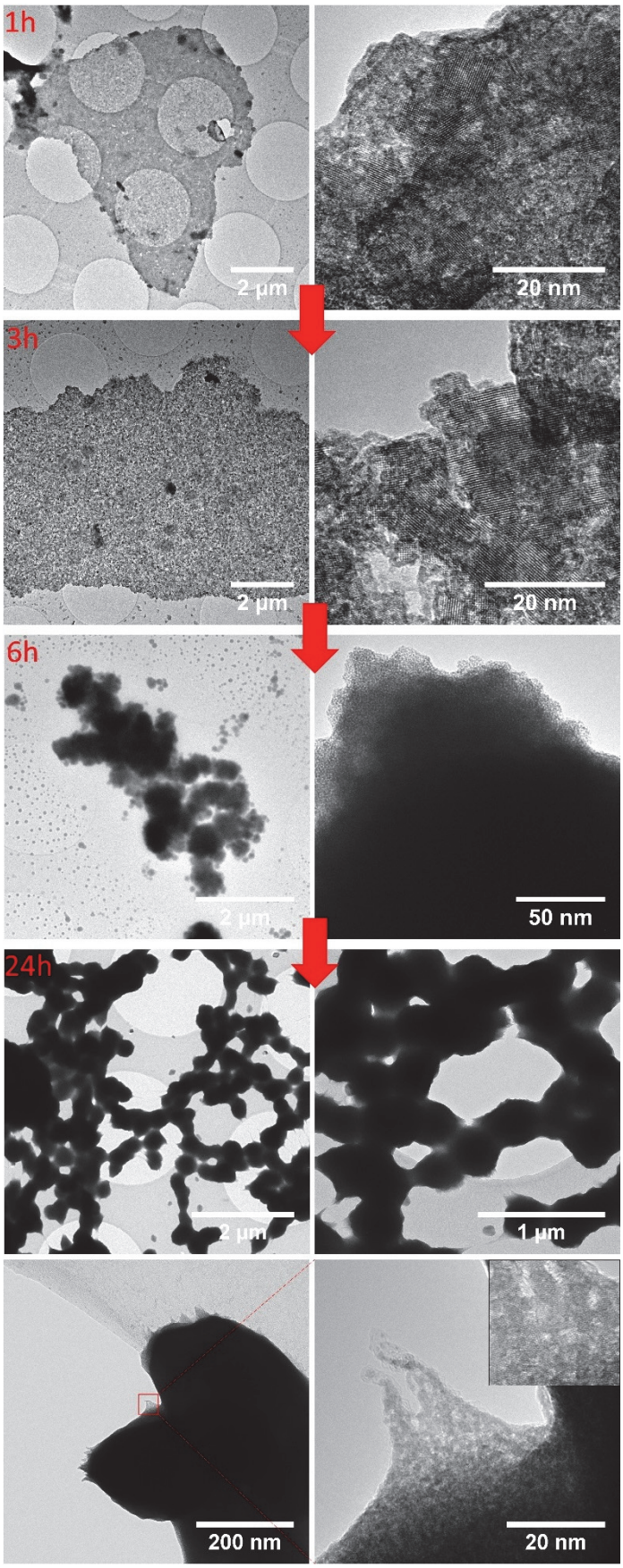

Figure S2. TEM images illustrating time evolution of the Re_2O_7-poly(THF) composite.

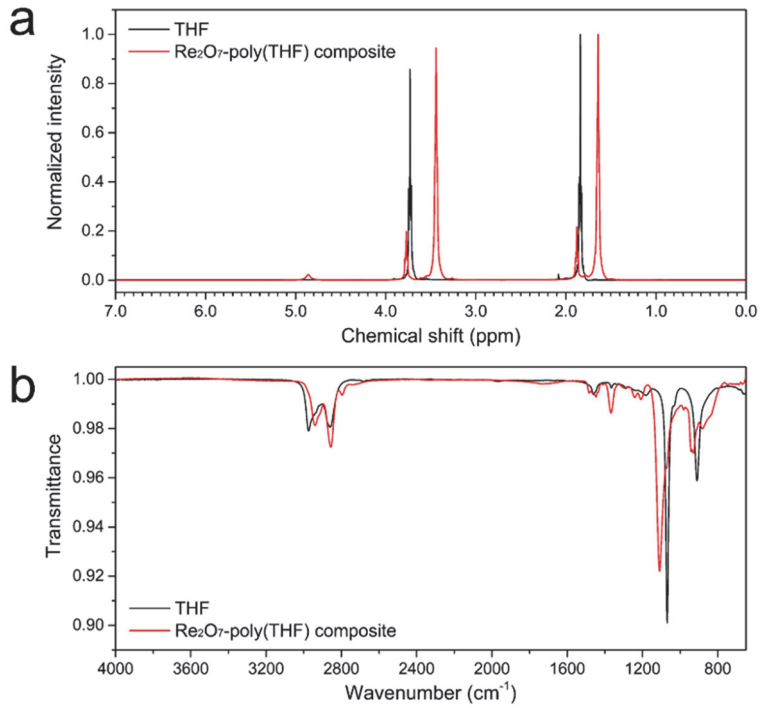

Figure S3. (a) ^{1}H-NMR and (b) FT-IR spectra of Re_2O_7-poly(THF) composite and THF.

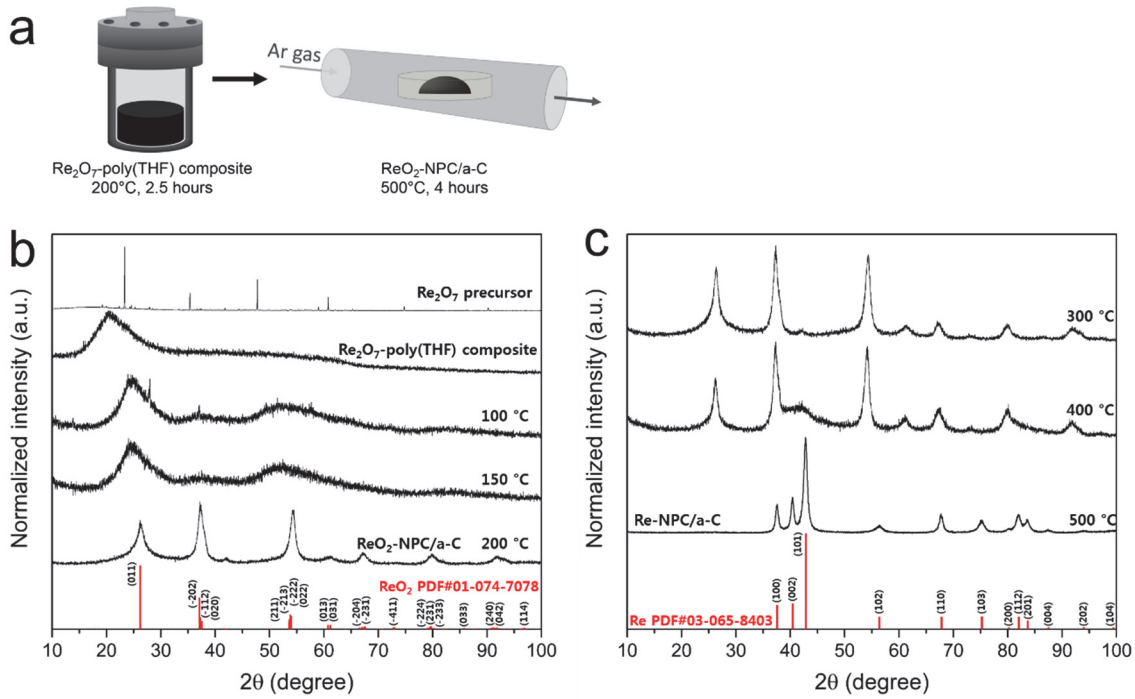

Figure S4. (a) Scheme of a two-step process converting "gels" of THF-crosslinked Re_2O_7 into Re nanoparticle/amorphous carbon clusters, Re-NPC/a-C. (b) PXRD spectra of Re_2O_7 precursor, Re_2O_7-poly(THF) composite gel, and solvothermally heated sample at different temperatures. (c) PXRD spectra of annealed ReO_2-NPC/a-C at different temperatures.

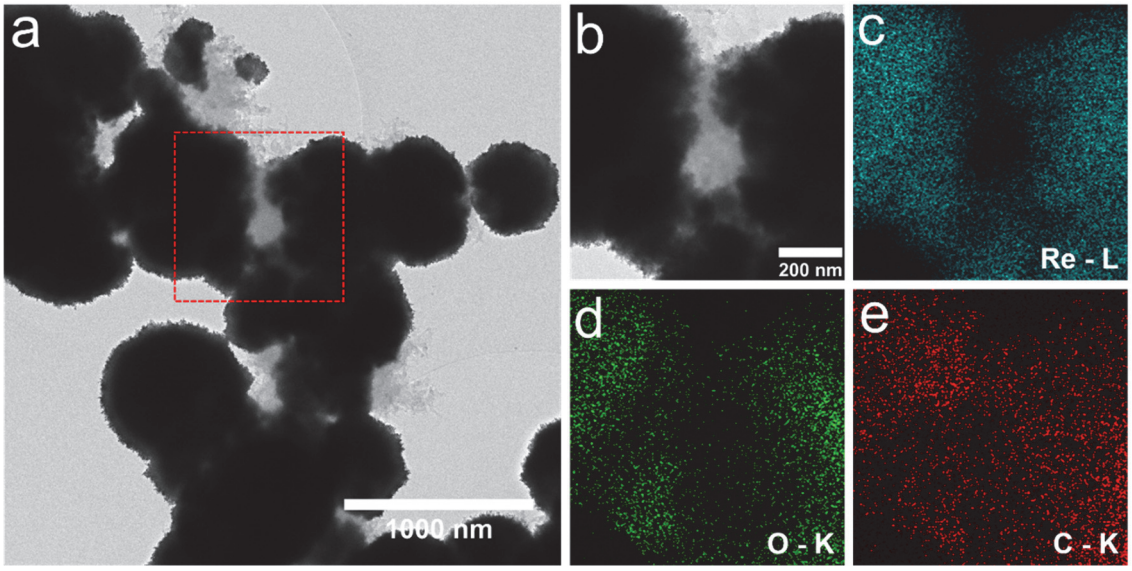

Figure S5. (a) TEM image of ReO_2-NPC/a-C. (b) Magnified image of ReO_2-NPC/a-C from area delineated in (a) by a red rectangle. Corresponding EDS mapping images for (c) Re, (d) O and (e) C.

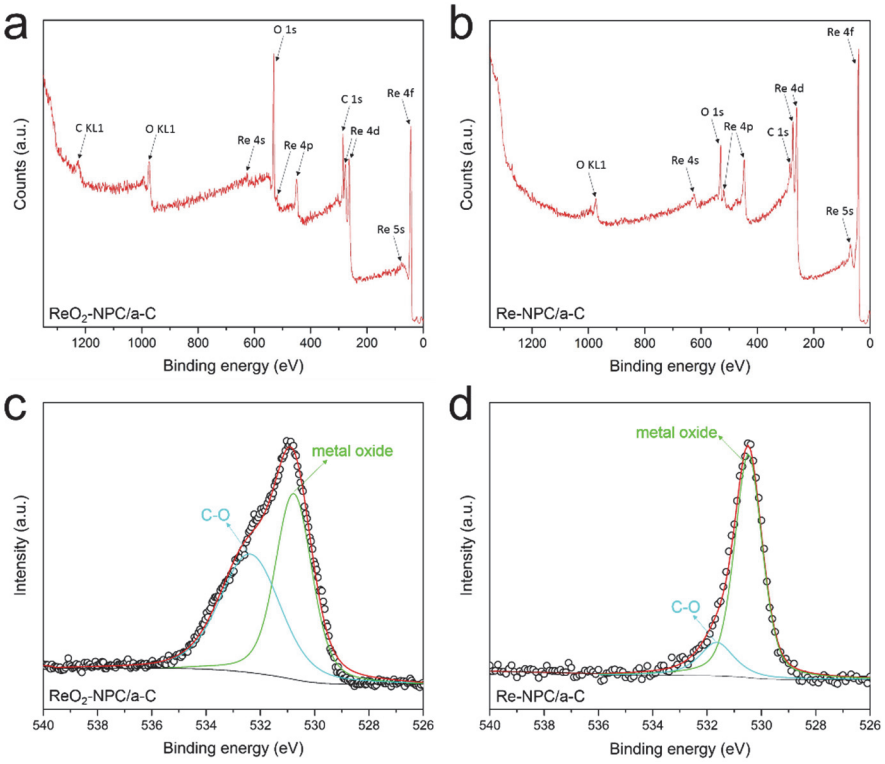

Figure S6. XPS survey scan of (a) ReO_2-NPC/a-C and (b) Re-NPC/a-C composites. Corresponding XPS spectra of oxygen band of (c) ReO_2-NPC/a-C and (d) Re-NPC/a-C.

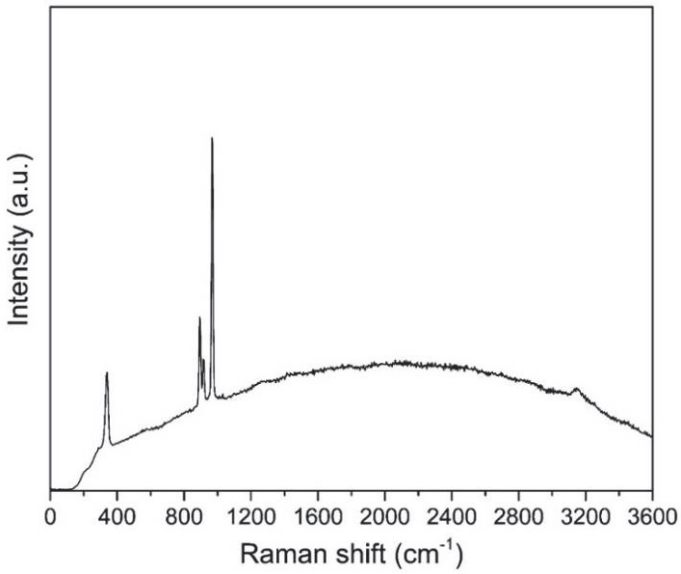

Figure S7. Raman spectrum of bulk Re powder purchased from Alfa Aesar (99.999%).

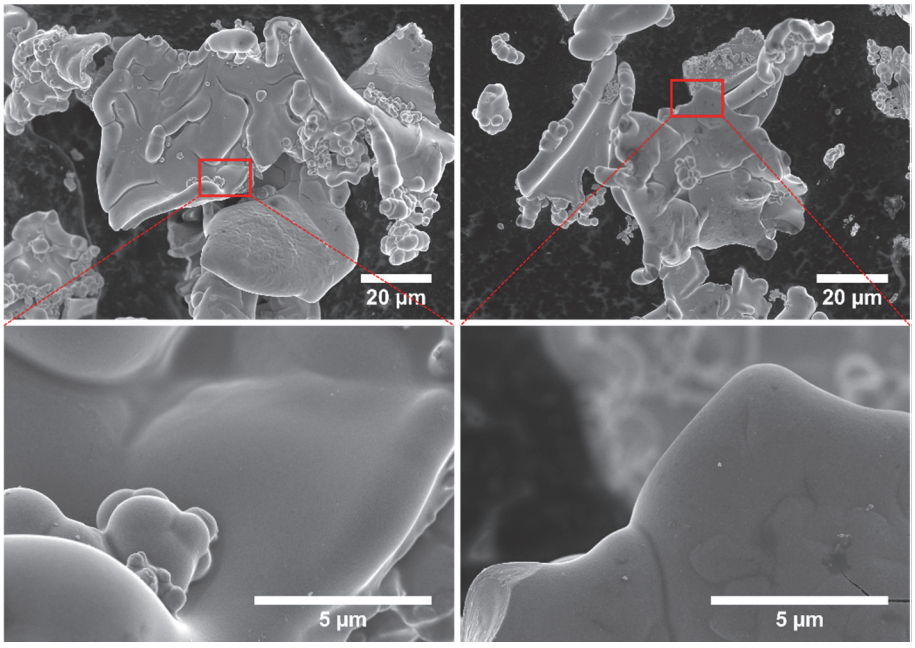

Figure S8. SEM images of bulk Re powder purchased from Alfa Aesar (99.999%).

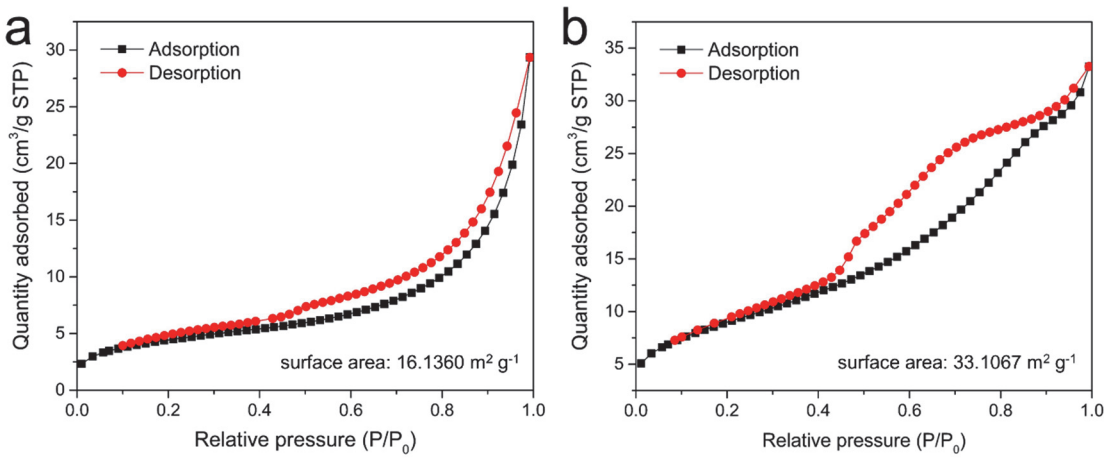

Figure S9. Brunauer–Emmett–Teller (BET) adsorption/desorption isotherms of (a) ReO_2-NPC/a-C and (b) Re-NPC/a-C nanocomposites.

Table S1.

Catalyst	Catalyst loading amount	Current density (*j*) [mA cm^{-2}]	Overpotential at corresponding *j* [mV]	Tafel slope [mV decade^{-1}]	Scan rate [mV s^{-1}]	Media	Reference
Re-NPC/a-C	0.283 mg cm^{-2}	10 10 10	133 122 164	56.3 53.8 69.6	2	0.5 M H_2SO_4 1M KOH 1M PBS	This work
Re-NPC/a-C /MWNT	0.283 mg cm^{-2}	10 10 10	107 107 163	43.5 50.7 69.2	2	0.5 M H_2SO_4 1M KOH 1M PBS	This work
Re/SiNW-31.1[a)]	0.411 mg cm^{-2}	10 10	~302 (initial) 209 (after 3000 cycles)	-- (initial) 81 (after 3000 cycles)	5	0.5 M H_2SO_4	[S1]
Rhenium wire	Geometric area 0.161 cm^2	10	~324	62.6	1	0.5 M H_2SO_4	[S2]
Rhenium wire	Geometric area 0.161 cm^2	40	360[b)]	62.6	1	0.5 M H_2SO_4	[S3]
p-Si(100)/ Re[c)]	--	5	200	--	10	0.1 M H_2SO_4	[S4]
poly-Re	--	10	~336	66	1	0.5 M H_2SO_4	[S5]

[a)]The overpotential and Tafel slope are possibly overestimated due to the catalyst being contaminated by Pt (because Pt counter electrode was used in acid electrolyte); [b)]Measured parameters were obtained only by cyclic voltammetry with fast scan rate of 500 mV s^{-1}; [c)]Study for photo-assisted HER electrocatalytic behavior of p-Si(100)/Re composite electrode.

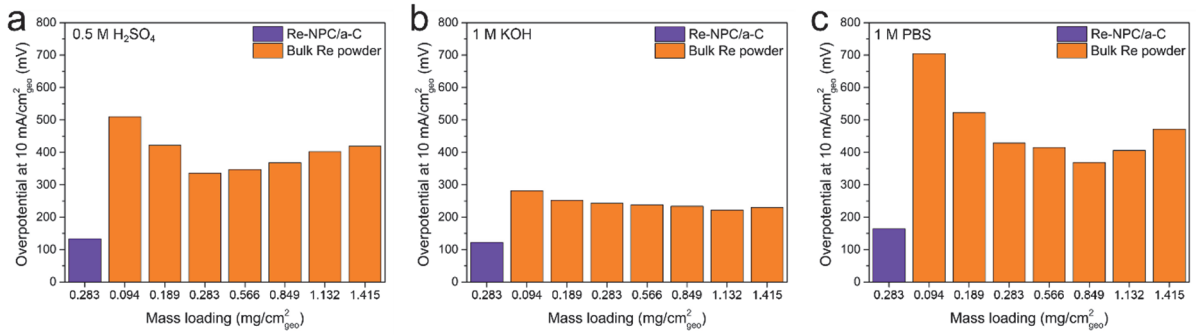

Figure S10. Overpotential comparisons of Re-NPC/a-C vs. different mass loadings of the bulk Re powder in (a) 0.5 M H_2SO_4, (b) 1 M KOH, and (c) 1 M PBS.

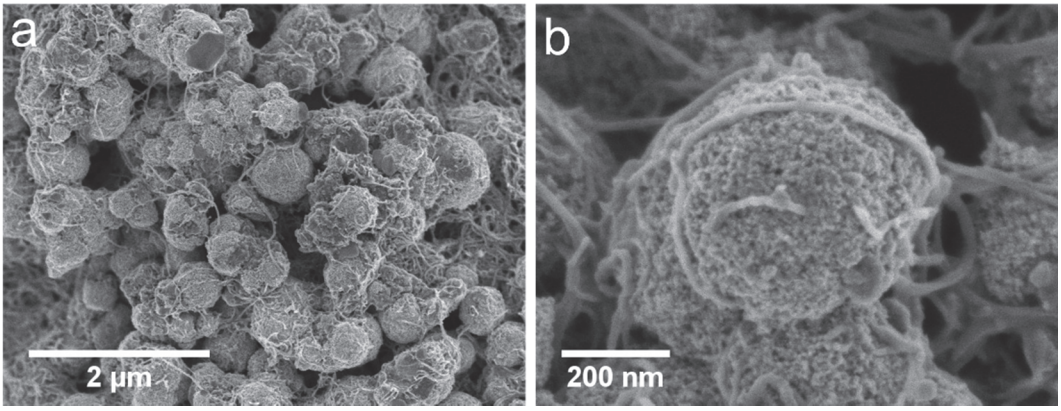

Figure S11. SEM image of Re-NPC/a-C/MWNT at (a) low magnification and (b) high magnification.

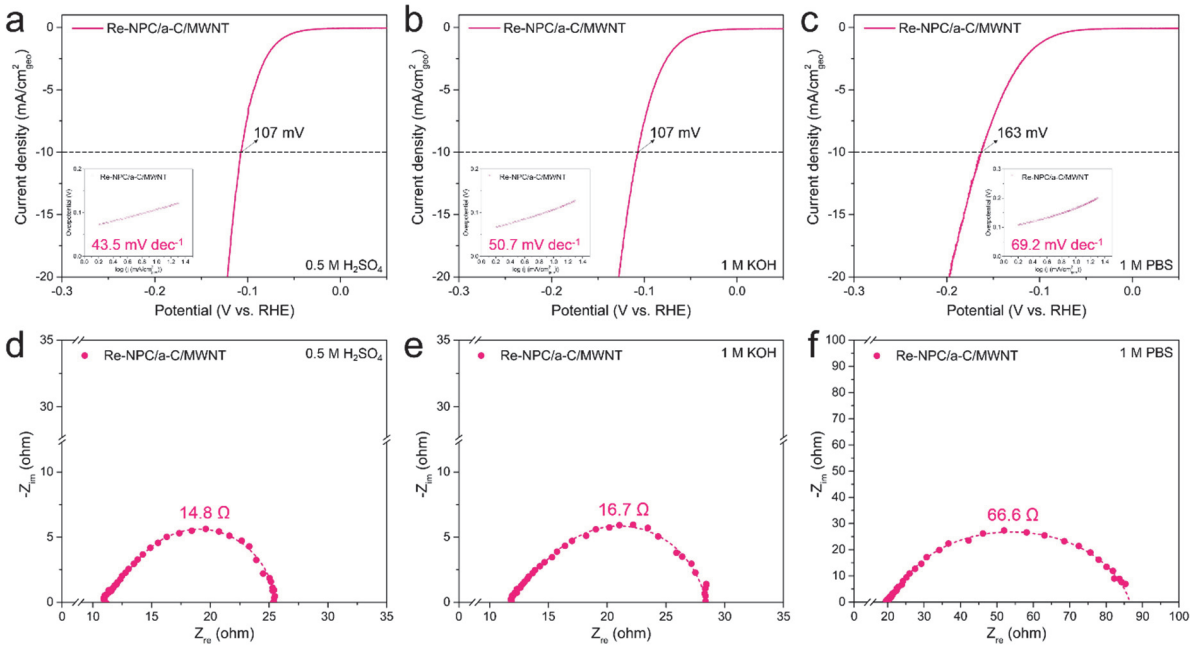

Figure S12. Polarization curves of Re-NPC/a-C/MWNT in (a) 0.5 M H_2SO_4, (b) 1 M KOH, and (c) 1 M PBS aqueous solution (inset: corresponding Tafel plot). Electrochemical impedance spectra of Re-NPC/a-C/MWNT at overpotential 0.17 V versus RHE and with alternating current (AC) amplitude of 5 mV in (d) 0.5 M H_2SO_4, (e) 1 M KOH, and (f) 1 M PBS.

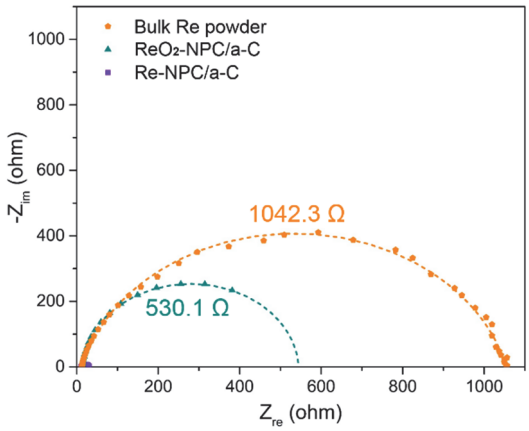

Figure S13. Electrochemical impedance spectra of different electrodes at overpotential 0.17 V versus RHE in 0.5 M H_2SO_4.

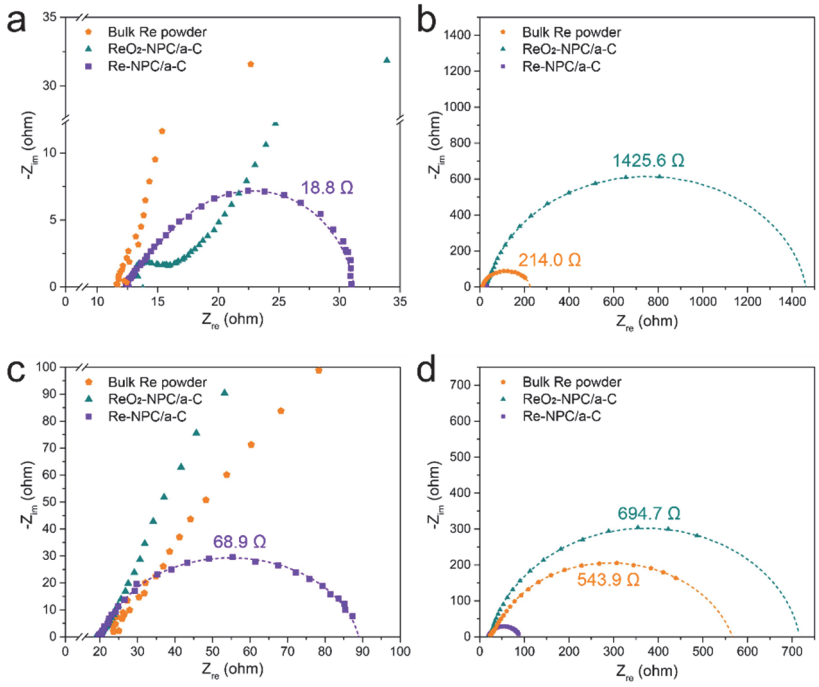

Figure S14. (a) Electrochemical impedance spectra of different electrodes at overpotential 0.17 V versus RHE in 1 M KOH and (b) Full impedance spectrum curves including bulk Re powder and ReO_2-NPC/a-C in 1 M KOH. (c) Electrochemical impedance spectra of different electrodes at overpotential 0.17 V versus RHE in 1 M PBS and (d) Full impedance spectrum curves including bulk Re powder and ReO_2-NPC/a-C in 1 M PBS.

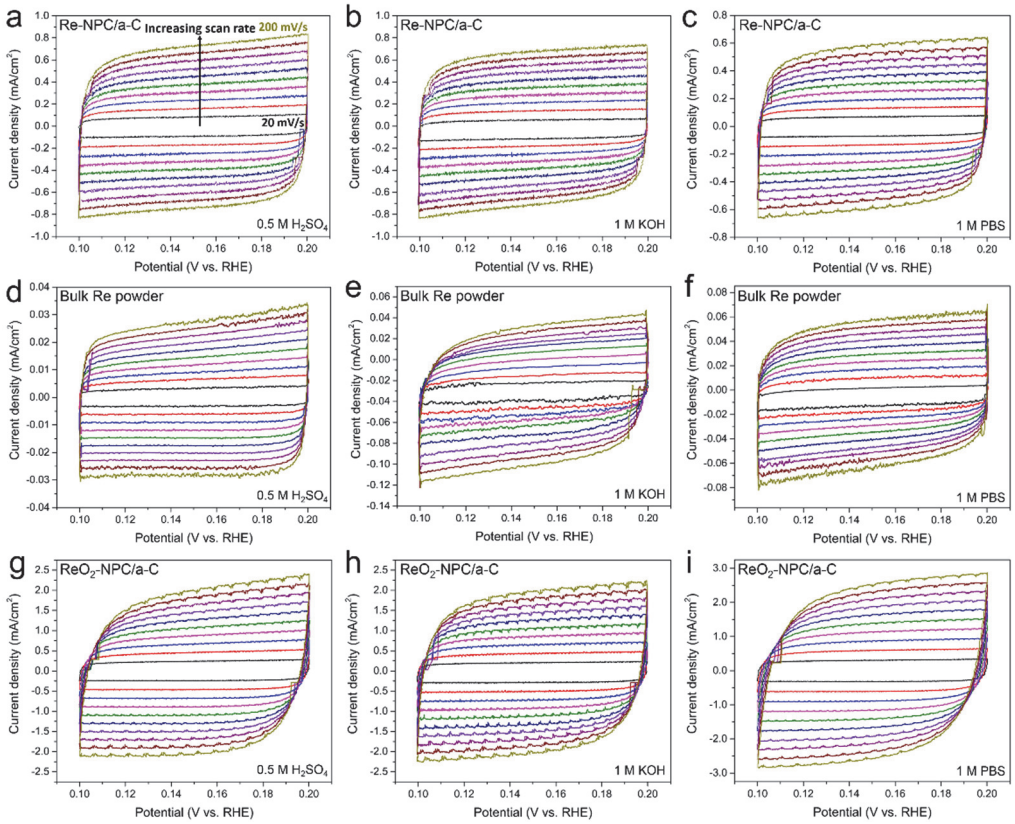

Figure S15. Cyclic voltammetry curves recorded at different scan rate (from 20 mV/s to 200 mV/s). Re-NPC/a-C in (a) 0.5 M H_2SO_4, (b) 1 M KOH, and (c) 1 M PBS. Bulk Re powder in (d) 0.5 M H_2SO_4, (e) 1 M KOH, and (f) 1 M PBS. ReO_2-NPC/a-C in (g) 0.5 M H_2SO_4, (h) 1 M KOH, and i) 1 M PBS.

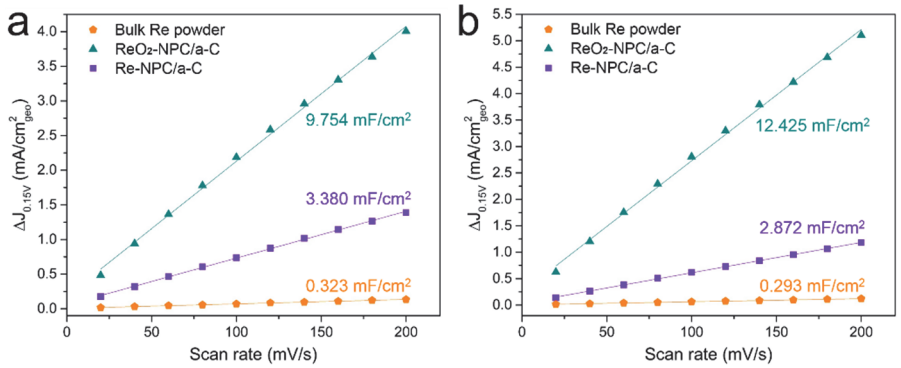

Figure S16. Capacitive current measured by CV at 0.15 V vs. RHE ($\Delta J_{0.15V}$), plotted as a function of scan rate in (a) 1 M KOH and (b) 1 M PBS.

Table S2.

Catalyst	C_{dl}[a] [mF cm^{-2}]	C_s [mF cm^{-2} per cm$^2_{ECSA}$]	ECSA [cm^2]	Overpotential at 1 mA cm$^{-2}_{ECSA}$ [mV]	Tafel slope [mV decade^{-1}]	Media
Bulk Re powder	0.136	0.035	3.886	269	100.6	0.5 M H_2SO_4
Re-NPC/a-C	3.595	0.035	102.714	217	68.8	
Bulk Re powder	0.323	0.040	8.075	230	78.4	1 M KOH
Re-NPC/a-C	3.380	0.040	84.500	217	70.5	
Bulk Re powder	0.293	0.040	7.325	358	111.9	1 M PBS
Re-NPC/a-C	2.872	0.040	71.8	338	111.8	

[a]Although it is not necessarily meaningful to directly compare the C_{dl} values for different materials[S6,S7], we note that our ReO_2-NPC/a-C composite has larger C_{dl} values (9.901 mF cm^{-2} in acidic, 9.754 mF cm^{-2} in basic, and 12.425 mF cm^{-2} in neutral electrolytes) due to more abundant amorphous carbon contents (~10 wt% of carbon from Elemental Analysis) than Re-NPC/a-C (~2 wt% of carbon from Elemental Analysis).

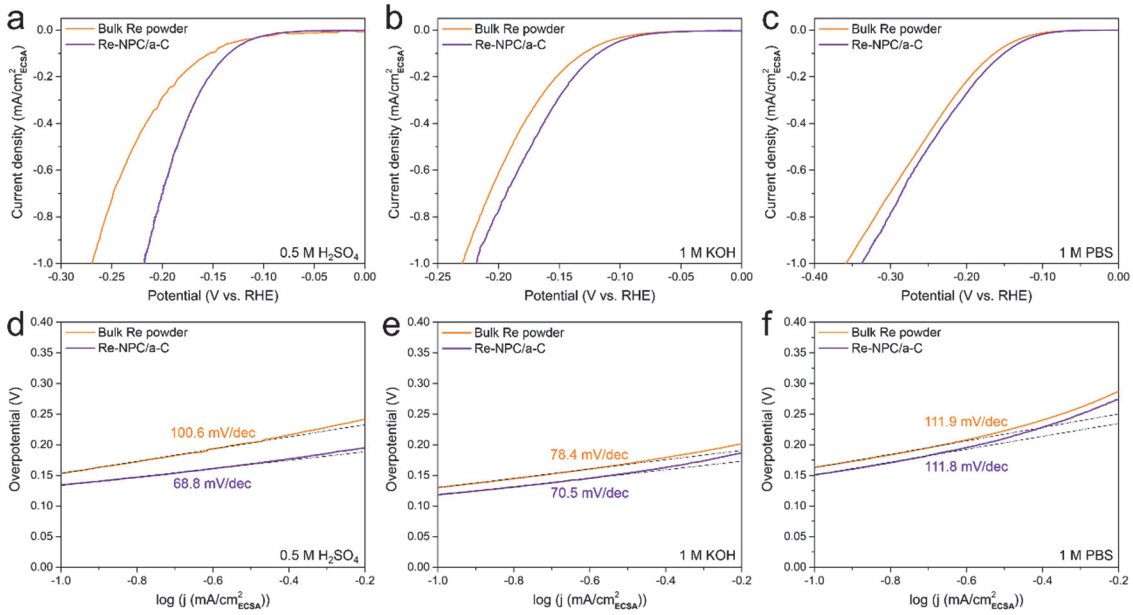

Figure S17. Polarization curves of bulk Re powder and Re-NPC/a-C normalized to the electrochemical active surface area (ECSA) in (a) 0.5 M H_2SO_4, (b) 1 M KOH, and (c) 1 M PBS. Corresponding Tafel plot in (d) 0.5 M H_2SO_4, (e) 1 M KOH, and (f) 1 M PBS.

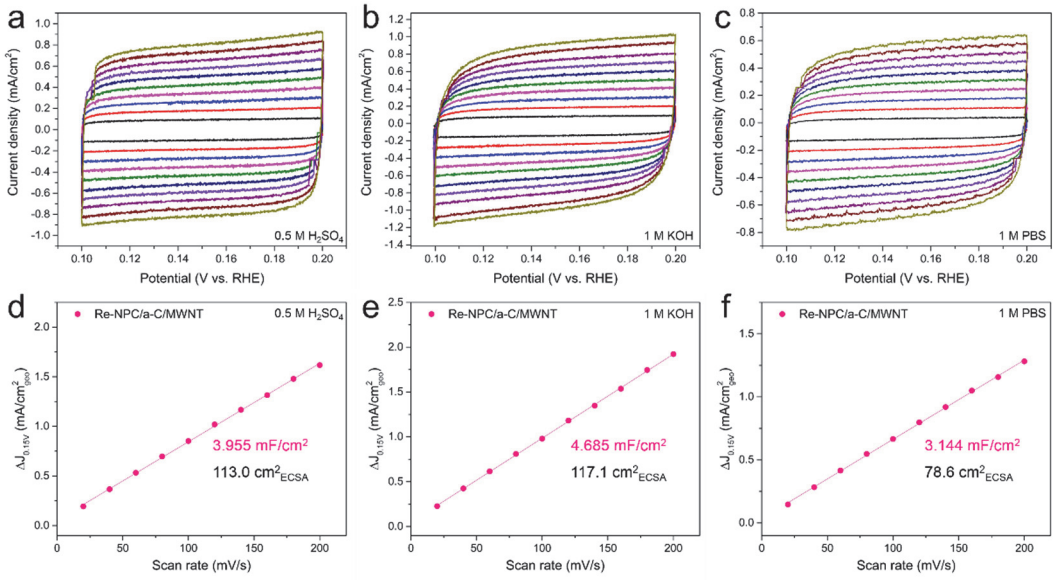

Figure S18. Cyclic voltammetry curves of Re-NPC/a-C/MWNT recorded at different scan rate (from 20 mV/s to 200 mV/s) in (a) 0.5 M H_2SO_4, (b) 1 M KOH, and (c) 1 M PBS. Capacitive current measured by CV at 0.15 V vs. RHE ($\Delta J_{0.15V}$), plotted as a function of scan rate in (d) 0.5 M H_2SO_4, (e) 1 M KOH, and (f) 1 M PBS (corresponding C_{dl} and ECSA values are indicated next to the curves).

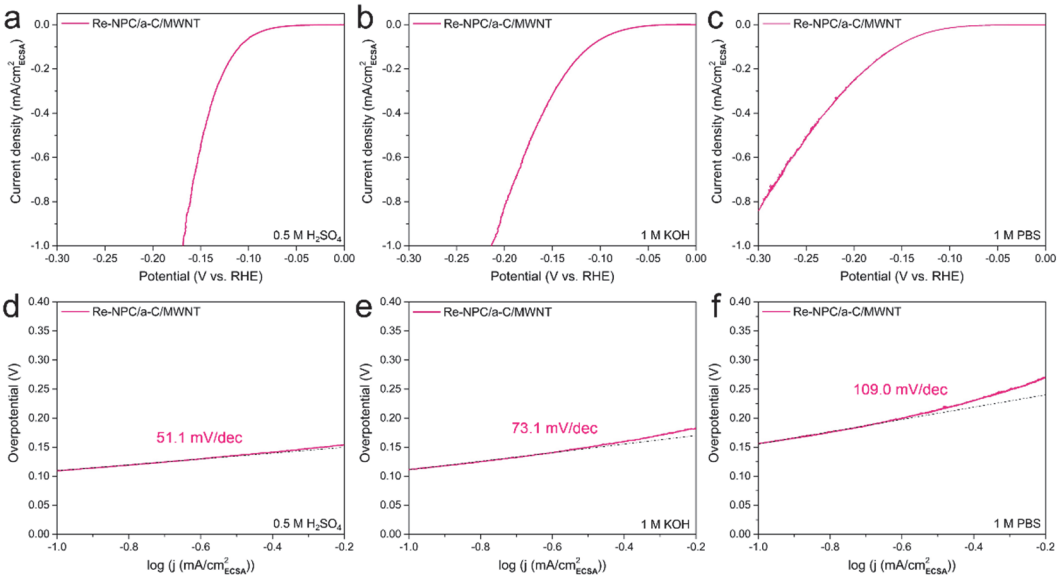

Figure S19. Polarization curves of Re-NPC/a-C/MWNT normalized to the electrochemical active surface area (ECSA) in (a) 0.5 M H_2SO_4, (b) 1 M KOH, and (c) 1 M PBS. Corresponding Tafel plots in (d) 0.5 M H_2SO_4, (e) 1 M KOH, and (f) 1 M PBS.

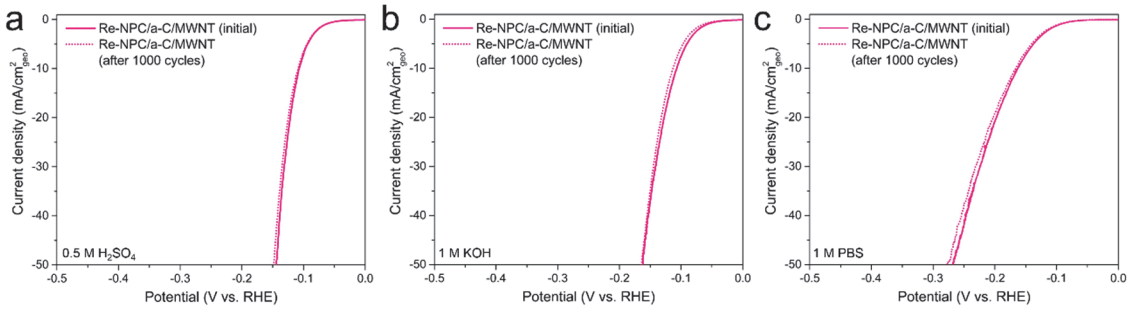

Figure S20. Polarization curves of Re-NPC/a-C/MWNT after preparation (solid lines) and after 1000 CV cycles (dotted lines) in (a) 0.5 M H_2SO_4, (b) 1 M KOH, and (c) 1 M PBS.

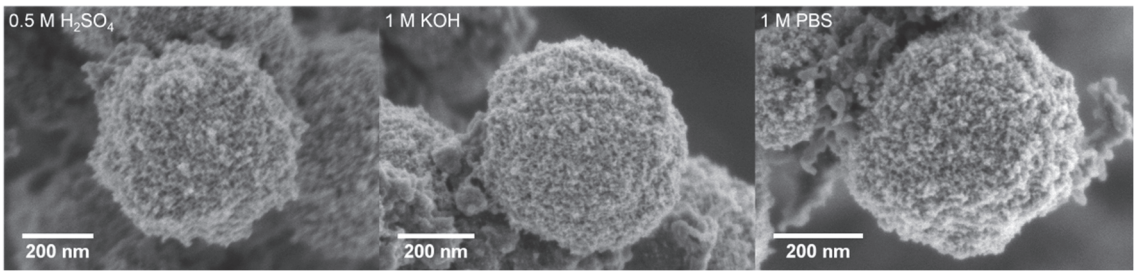

Figure S21. SEM images of Re-NPC/a-C after HER process (1000 CV cycles) in different electrolytes.

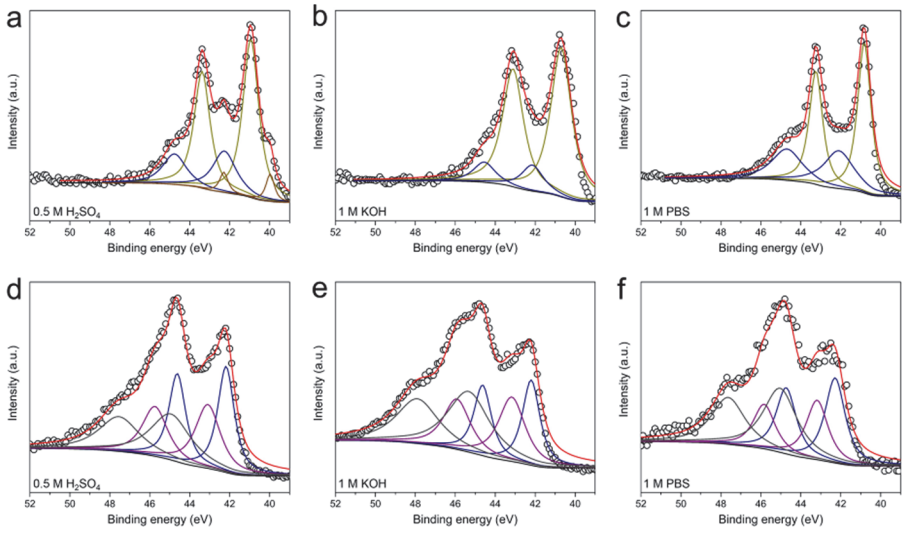

Figure S22. Re 4f XPS spectra of Re-NPC/a-C after HER process (1000 CV cycles) in (a) 0.5 M H_2SO_4, (b) 1 M KOH, and (c) 1 M PBS. Re 4f XPS spectra of ReO_2-NPC/a-C after HER process (1000 CV cycles) in (d) 0.5 M H_2SO_4, (e) 1 M KOH, and (f) 1 M PBS.

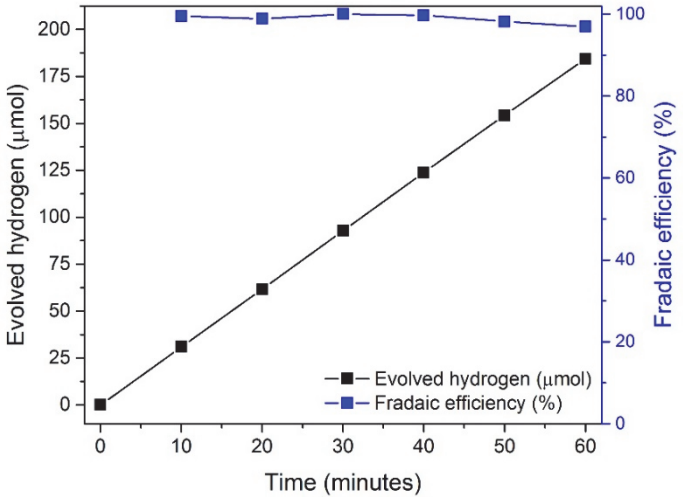

Figure S23. The amounts of experimentally evolved hydrogen for Re-NPC/a-C at 10 mA/cm^2 current density for 60 minutes (black dot, left y-axis) and corresponding Faradaic efficiency based on theoretically calculated value (blue dot, right y-axis).

Supplementary References:

[S1] Yang, L.; Lu, S.; Wang, H.; Shao, Q.; Liao, F.; Shao, M. The Self-Activation and Synergy of Amorphous Re Nanoparticle–Si Nanowire Composites for the Electrocatalytic Hydrogen Evolution. *Electrochim. Acta* **2017**, *228*, 268-273.

[S2] Garcia-Garcia, R.; Rivera, J. G.; Antaño-Lopez, R.; Castañeda-Olivares, F.; Orozco, G. Impedance Spectra of the Cathodic Hydrogen Evolution Reaction on Polycrystalline Rhenium. *Int. J. Hydrogen Energy* **2016**, *41*, 4660-4669.

[S3] Garcia-Garcia, R.; Ortega-Zarzosa, G.; Rincón, M. E.; Orozco, G. The Hydrogen Evolution Reaction on Rhenium Metallic Electrodes: a Selected Review and New Experimental Evidence. *Electrocatalysis* **2015**, *6*, 263-273.

[S4] Muñoz, E. C.; Schrebler, R. S.; Orellana, M. A.; Córdova, R. Rhenium Electrodeposition Process onto p-Si (100) and Electrochemical Behaviour of the Hydrogen Evolution Reaction onto p-Si/Re/0.1 M H_2SO_4 Interface. *J. Electroanal. Chem.* **2007**, *611*, 35-42.

[S5] Chun, J. H.; Jeon, S. K.; Ra, K. H.; Chun, J. Y. The Phase-Shift Method for Determining Langmuir Adsorption Isotherms of Over-Potentially Deposited Hydrogen for the Cathodic H_2 Evolution Reaction at Poly-Re/Aqueous Electrolyte Interfaces. *Int. J. Hydrogen Energy* **2005**, *30*, 485-499.

[S6] Li, J.-S.; Wang, Y.; Liu, C.-H.; Li, S.-L.; Wang, Y.-G.; Dong, L.-Z.; Dai, Z.-H.; Li, Y.-F.; Lan, Y.-Q. Coupled Molybdenum Carbide and Reduced Graphene Oxide Electrocatalysts for Efficient Hydrogen Evolution. *Nat. Commun.* **2016**, *7*, 11204.

[S7] Park, H.; Encinas, A.; Scheifers, J. P.; Zhang, Y.; Fokwa, B. P. Boron-Dependency of Molybdenum Boride Electrocatalysts for the Hydrogen Evolution Reaction. *Angew. Chem. Int. Ed.* **2017**, *56*, 5575-5578.